Rapid and highly-sensitive melamine sensing based on the efficient inner filter effect of Ag nanoparticles on the fluorescence of eco-friendly ZnSe quantum dots

ARTICLE *in* SENSORS AND ACTUATORS B CHEMICAL · JUNE 2014

Impact Factor: 4.1 · DOI: 10.1016/j.snb.2014.06.056

Sensors and Actuators B 202 (2014) 1175–1182

Contents lists available at ScienceDirect

Sensors and Actuators B: Chemical

journal homepage: www.elsevier.com/locate/snb

Rapid and highly-sensitive melamine sensing based on the efficient inner filter effect of Ag nanoparticles on the fluorescence of eco-friendly ZnSe quantum dots

Xianyi Cao [1], Fei Shen [1], Minwei Zhang, Chunyan Sun *

Department of Food Quality and Safety, Jilin University, Changchun 130062, China

ARTICLE INFO

Article history:
Received 10 April 2014
Received in revised form 6 June 2014
Accepted 15 June 2014
Available online 20 June 2014

Keywords:
Melamine
ZnSe quantum dots
Ag nanoparticles
Inner filter effect
Fluorescence
Detection

ABSTRACT

A very practical and competitive sensing strategy for melamine has been developed based on the efficient inner filter effect (IFE) of Ag nanoparticles (AgNPs) on the fluorescence of eco-friendly ZnSe quantum dots (QDs). The fluorescence emission of ZnSe QDs could be quenched significantly by AgNPs *via* IFE, which resulted in a fluorescence "off-state". The presence of melamine could induce the aggregation of AgNPs and modulate the IFE process. Thus the IFE-decreased fluorescence could gradually recover in a melamine concentration-dependent way, thereby achieving the fluorescence "turn-on" sensing for melamine. The detection mechanism was clearly illustrated and the influences of various experimental conditions were also investigated. Under the optimal conditions, a decent linear relationship for melamine was obtained in the range from 1.0 to 36 $\mu g\,L^{-1}$, and the detection limit was as low as 0.11 $\mu g\,L^{-1}$. The IFE-based strategy was successfully applied for melamine analysis in raw milk and egg samples and satisfactory results have been achieved. Therefore, it is very promising to use this simple, rapid, sensitive and eco-friendly method for on-site and real-time screening of melamine.

1. Introduction

Melamine, also known as tripolycyanamide, is a basic organic chemical raw material with a chemical formula of $C_3H_6N_6$ (the molecular structure is shown in Scheme 1A). It has been extensively used in the manufacture of polymer resins for plastics, coatings, adhesives, glues and laminates, but banned in food products. However, because of its high nitrogen content (66% by mass) and low cost, melamine was illegally adulterated to raw milk and animal feed to falsely increase the apparent crude protein content, since the traditional Kjeldahl method cannot identify nitrogen source [1]. In addition, melamine can also be detected in eggs as a metabolite and degradation product of cyromazine, since cyromazine is often employed as a feed additive for laying hens to prevent flies from hatching in their manure [2]. Melamine alone has low oral acute toxicity. However, it can form insoluble reticulate crystal in urinary system with its *in vivo* hydrolysate, cyanuric acid, or with uric acid [3]. Thus, due to the nephrotoxicity, a long-term melamine intake may result in illnesses and even deaths of infants and pets [4]. For the purpose of protecting consumer health, developing excellent methods for melamine analysis in daily foods has become very urgent and essential.

Up to now, various analytical methods for melamine have been reported. Traditional strategies, including high-performance liquid chromatography (HPLC) [5], liquid chromatography–tandem mass spectrometry (LC–MS/MS) [6], gas chromatography–mass spectrometry (GC–MS) [7], enzyme-linked immunosorbent assay (ELISA) [8], near-infrared spectroscopy (NIR) [9] and capillary zone electrophoresis (CZE) [10], have high sensitivity, selectivity and reliability. However, most of them require expensive instruments, professional operators, complicated sample pretreatment procedures, or widespread use of harmful organic solvents. Some novel methods, such as electrochemistry [11], chemiluminescence [12], fluorimetry [13], surface enhanced Raman spectroscopy (SERS) [14] and colorimetry based on polydiacetylene liposomes [15] have also been developed, but most of them still suffer from poor sensitivity, high cost or complicated chemical synthesis. Therefore, developing a rapid, simple, sensitive, eco-friendly method for melamine analysis is of great importance and urgency. With the rapid development of nanotechnology, metal nanoparticles (NPs) as colormetric probes, especially Au nanoparticles (AuNPs) and Ag nanoparticles (AgNPs), have attracted extensive attention due to their unique size-dependent and interparticle

* Corresponding author. Tel.: +86 431 87836375; fax: +86 431 87836391.
E-mail addresses: sunchuny@jlu.edu.cn, sunchunyan1977@163.com (C. Sun).
[1] These authors contributed equally to this work.

http://dx.doi.org/10.1016/j.snb.2014.06.056
0925-4005/

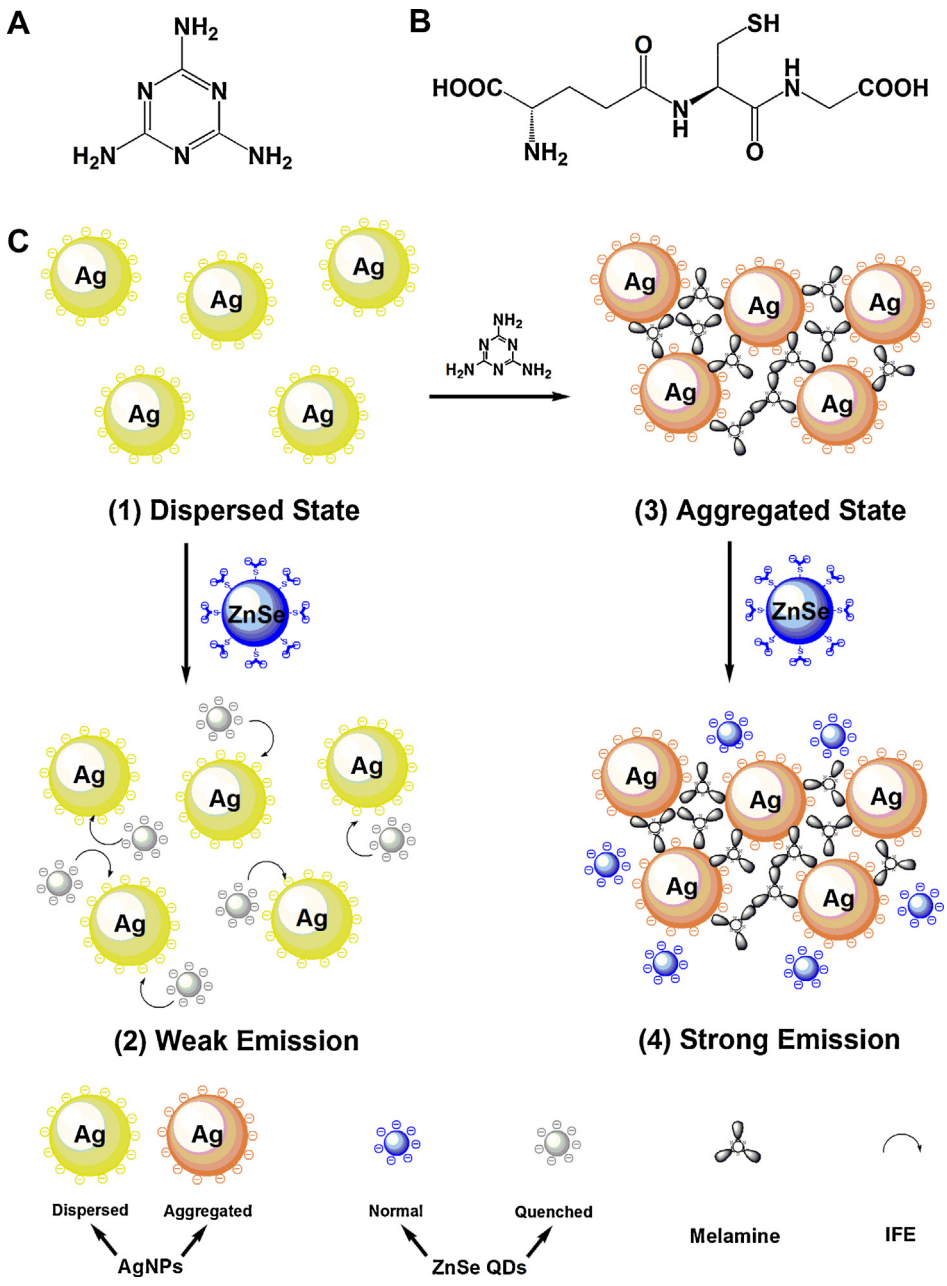

Scheme 1. The molecular structures of melamine (A) and L-GSH (B); Schematic illustration of the "turn-on" fluorescent detection of melamine based on the IFE of AgNPs on ZnSe QDs (C). (For interpretation of the references to color in text, the reader is referred to the web version of the article.)

distance-dependent optical properties [16,17]. The molecular recognition between AuNPs/AgNPs and analytes would be rapidly transformed into solution color change, which could be readily observed by naked eyes without any sophisticated equipment. Thus, it has been widely applied for detection of vaious ions [18,19] and small molecules [20,21], including melamine [22,23]. However, the sensitivity of these colorimetric methods is still less than satisfactory.

Quantum dots (QDs), a kind of semiconductor nanoclusters, have revealed significant superiorities for their application in chemistry, physics and life science, because they possess unique optical properties, such as high fluorescence quantum yield (QY), excellent stability against photobleaching and size-controlled luminescence [24]. Thus, they have been regarded as decent substitutes for traditional organic fluorescent dyes in fluorimetry. For example, some fluorimetric methods for detection of various analytes including melamine have been established based on fluorescence resonance energy transfer (FRET) between AuNPs (accepter) and QDs (donor) [25–27]. However, the formation of FRET process requires a particular distance between donors and accepters to ensure the valid interaction [28]. Therefore, the establishment of the above FRET-based sensors commonly demands complex surface chemical modification of AuNPs and QDs, which would distinctly undermine their practicality. Moreover, a serious drawback of the current QDs technology is its strong dependence on Cd-based QDs, which has brought in comprehensive environmental and safety concerns. The inherent heavy-metal property of Cd raises misgivings about its high carcinogenicity, potential chronic health risks and disposal hazards [29].

In the present work, a simple, sensitive, rapid and reliable sensing system for melamine was developed based on the inner filter effect (IFE) of citrate-stabilized AgNPs (absorber) on the fluorescence of ZnSe QDs (fluorophore) capped with L-glutathione (L-GSH). IFE refers to the absorption of the exciting radiation and/or

emitted fluorescence radiation of fluorophores by absorbers [30]. Although IFE is originally a source of errors in fluorimetry, several recent studies have explored its application in developing innovative fluorescent analyses [31–34]. Because the absorbance changes of the absorber are exponentially converted into the fluorescence changes of the fluorophore, an enhanced sensitivity can be achieved with respect to observing the absorbance changes alone [35]. Citrate-stabilized AgNPs were chosen to be the absorber due to their lower fabrication cost, flexibly-tunable absorption spectrum, extremely high molar extinction coefficient (ε) which is much larger than those of conventional dyes as well as the same-sized AuNPs [36,37]. Zn-based QDs, a type of wide band gap II–VI semiconductor nanoclusters, have been deemed to be a very promising alternative to Cd-based QDs, due to their properties of low cytotoxicity and intense blue luminescence [38,39]. In this study, water soluble L-GSH-capped ZnSe QDs were successfully synthesized using a facile and simple aqueous phase route, which is simpler, environmental-friendly and cost-effective than previous organometallic approaches [40]. In addition, it has been proved that L-GSH (the molecular structure is shown in Scheme 1B) as a capping ligand can effectively improve the QY, water-solubility and biocompatibility of QDs [40]. Therefore, L-GSH-capped ZnSe QDs were herein chosen to be an eco-friendly fluorophore. Thus, a high-efficiency IFE process was established in this study since a broad overlap was obtained between the absorption band of citrate-stabilized AgNPs and the emission band of L-GSH-capped ZnSe QDs. Besides, compared with previous FRET-based methods, this IFE-based approach does not require specific surface modification to adjust their interparticle distance between fluorophores and absorbers, making the sensor preparation much simpler [34].

To the best of our knowledge, this is the first report so far to study an IFE-based assay with AgNPs as absorber and QDs as fluorophore, as well as with eco-friendly Zn-based QDs as the fluorescent probe for melamine sensing. The principle of the present method is illuminated in Scheme 1C. Citrate-stabilized AgNPs solution was yellow and well-monodispersed (1). The fluorescence emission of ZnSe QDs could be obviously quenched by AgNPs *via* IFE (2). When added into AgNPs solution, melamine would strongly bind to the surface of AgNPs through its amine groups, inducing the monodispersed AgNPs to aggregate, accompanied with the absorption decrease around 395 nm and a yellow-to-red color change of the solution (3). Consequently, with the presence of melamine, the IFE of AgNPs on ZnSe QDs was impaired, making the fluorescence of ZnSe QDs recover (4). The fluorescence recovery efficiency exhibits a good linear dependence on melamine concentration in a wide range with high sensitivity. The proposed method was further successfully applied to detect melamine in real milk and egg samples with satisfactory results.

2. Experimental

2.1. Materials and reagents

Unless otherwise stated, all the chemicals were of analytical grade and used as received without further purification. Melamine and lactose were purchased from Aladdin Reagent Company (Shanghai, China). L-GSH was obtained from Sigma-Aldrich (St. Louis, USA). Se powder was obtained from Meixing Chemical Industry Co., Ltd. (Shanghai, China). $ZnAc_2{\cdot}2H_2O$, $CaCl_2$, and trichloroacetic acid were purchased from Xilong Chemical Co., Ltd. (Shantou, China). Sodium citrate, $AgNO_3$, NaOH, $NaBH_4$, H_3BO_3, $Na_2B_4O_7{\cdot}10H_2O$, NaCl, $MgCl_2$, KCl, HCl, KNO_3, glucose and vitamin C were purchased from Beijing Chemical Reagent Company (Beijing, China). Vitamin B_1, glycine, L-histidine, L-tryptophan, L-threonine and L-lysine were obtained from Huishi Biochemical Reagent Company (Shanghai, China). Acetonitrile was purchased from Yuwang Chemical Reagent Company (Yucheng, China). High purity N_2 (99.999%) and double distilled water (DDW) were used throughout the whole assay. 2 mM borate buffer solution (pH = 8) was prepared for further use. Different brands of raw milk and egg samples were purchased from a local supermarket.

2.2. Apparatus

All optical measurements were carried out at room temperature. Absorption spectra were recorded on a 2550 UV–vis spectrophotometer (Shimadzu, Tokyo, Japan). Fluorescence spectra were acquired on a RF-5301PC fluorescence spectrophotometer (Shimadzu, Tokyo, Japan) whose excitation and emission slits were both set at 5 nm. High resolution transmission electron microscopy (HRTEM) measurements were carried out on a TECNAI F20 (FEI Co., Eindhoven, The Netherlands) operated at an accelerating voltage of 200 kV. Fluorescence lifetime measurements were conducted by using a FLS 920 spectrometer (Edinburgh Instruments, Livingston, UK). Zeta potential (ζ) measurements were performed on a Zeta-Sizer Nano ZS90 particle size analyzer (Malvern, Worcestershire, UK). Centrifugation was performed on a CR20B2 refrigerated centrifuge (Hitachi, Tokyo, Japan). Homogenization was performed on a WH-3 vortex mixer (Huxi, Shanghai, China). All pH measurements were carried out with a Model pHS-3C (Chenghua, Shanghai, China).

2.3. Synthesis of L-GSH-capped ZnSe QDs

Water-soluble L-GSH-capped ZnSe QDs were prepared according to the procedure reported by Zheng et al. with minor modifications [40]. The whole synthetic process was carried out under the protection of N_2. Briefly, 0.014 g $NaBH_4$ and 0.0078 g Se powder were mixed in 300 μL DDW in ice-bath. Se powder was completely reduced by $NaBH_4$ 40 min later and NaHSe solution was obtained. Zn precursor solution was prepared by mixing 0.088 g $ZnAc_2{\cdot}2H_2O$ and 0.12 g L-GSH in 100 mL DDW, followed by adjusting pH to 11 using 1 M NaOH. Then 300 μL of freshly prepared NaHSe solution was added into the Zn precursor solution under continuous stirring. The mixture was heated to 95 °C, incubated for 90 min and naturally cooled down to room temperature. To remove excess Zn^{2+}–L-GSH complex and other impurities, the as-prepared ZnSe QDs were precipitated and washed twice with ethanol, and the precipitation was thoroughly dried in vacuum. Finally, the L-GSH-capped ZnSe QDs stock solution was obtained by redissolving the precipitation in 100 mL DDW. The final concentration of the ZnSe QDs was 1 mM according to the initial Se^{2-} concentration and the stock solution was kept in dark at 4 °C.

QY indicates the efficiency of a fluorescent material in converting the excitation into fluorescent emission. The gradient method was adopted to estimate the photoluminescence QY of L-GSH-capped ZnSe QDs [41,42], by using L-tryptophan (L-Trp, QY = 13%, in water, 20 °C) as a reference and exciting all the samples at 300 nm. Specifically, the QY of L-GSH-capped ZnSe QDs was calculated from the following equation:

$$QY_{ZnSe} = QY_{L-Trp} \cdot \frac{m_{ZnSe}}{m_{L-Trp}} \quad (1)$$

where m is the slope of integrated fluorescence intensity *versus* absorbance at 300 nm. The integrated fluorescence intensity was obtained by integrating the emission intensity over the entire wavelength range under the emission peak, and the absorbance was kept between 0.01 and 0.1 to avoid the self-absorption effect [43].

The nanocluster feature of L-GSH-capped ZnSe QDs could be tuned by adopting different reaction conditions. In the present work, the molar ratio of Zn:Se: L-GSH, the concentration of $ZnAc_2$,

the reaction temperature and the pH were optimized to be 4:1:4, 4 mM, 95 °C, and 11 respectively, which resulted in relatively high QY of 28.6% and good analytical performance of ZnSe QDs in this assay.

2.4. Synthesis of citrate-stabilized AgNPs

Citrate-stabilized AgNPs were prepared according to a previously reported procedure with some modifications [44]. All glassware was soaked in freshly prepared aqua regia for 24 h, rinsed completely and dried thoroughly prior to use. 3 mL of 10 mM $NaBH_4$ was dropwise added to 100 mL of 0.25 mM $AgNO_3$ and 0.25 mM sodium citrate under virogous stirring. The reaction was held for 20 min at room temperature and a yellow AgNPs colloidal solution was obtained. The mixture was left undisturbedly for 8 h, and then stored at 4 °C for further use.

The size and morphology of the AgNPs were characterized with HRTEM and the average particle diameter is observed to be 10 nm. ε of the as-preapred 10 nm AgNPs was approximately calculated to be 6.9×10^8 M^{-1} cm^{-1} by the following Mie-theory-based formula proposed by Navarro and Werts [45]:

$$\varepsilon = Ad^{\gamma} \begin{cases} A = 2.3 \times 10^5 \ M^{-1}\,cm^{-1}, & \gamma = 3.48, \quad d \le 38\,nm \\ A = 4.2 \times 10^8 \ M^{-1}\,cm^{-1}, & \gamma = 0.77, \quad d > 38\,nm \end{cases} \quad (2)$$

where d is the average diameter of AgNPs. Thus, according to Lambert-Beer's law, the molar concentration of the AgNPs was calculated to be 3.9 nM.

2.5. Analytical method

A quartz cuvetter (10 mm × 10 mm × 40 mm) was used for loading test samples. Briefly, 0.3 mL of 2 mM borate buffer solution (pH = 8) was added into 1 mL of 3.9 nM AgNPs solution. Then the mixture was respectively mixed with 1.2 mL of different concentrations of melamine and incubated for 16 min. After that, 0.5 mL of 1 mM ZnSe QDs solution was added into the above solution and mixed thoroughly. The fluorescence emission intensity of the solution was recorded at 370 nm with the excitation wavelength of 300 nm. The calibration curve for melamine was set up by $(F - F_0)/F_0$ *versus* the concentration of melamine, where F and F_0 are the fluorescence intensity of the system in the presence and absence of melamine, respectively.

2.6. Detection of melamine in real samples

Raw milk and egg samples were spiked with different concentrations of melamine. Then 15 mL of 1% (*w*/*v*) trichloroacetic acid and 5 mL of acetonitrile were added into 2.0 g of each spiked sample. After homogenized, vibratingly extracted and centrifuged at 6000 rpm for 10 min respectively, the supernatant was filtered through a piece of filter paper soaked by 1% (*w*/*v*) trichloroacetic acid. The filtrate was diluted to 25 mL with 1% (*w*/*v*) trichloroacetic acid to obtain the testing sample solution for fluorescence analysis according to the method in Section 2.5.

3. Results and discussion

3.1. Characteristics of L-GSH-capped ZnSe QDs and citrate-stabilized AgNPs

The normalized UV–vis absorption and fluorescence emission spectra of the obtained L-GSH-capped ZnSe QDs are respectively shown as a and b in Fig. 1A. An absorption peak is observed around 355 nm and the fluorescence emission maximum can be achieved at 370 nm. Besides, it can be seen that the fluorescence emission

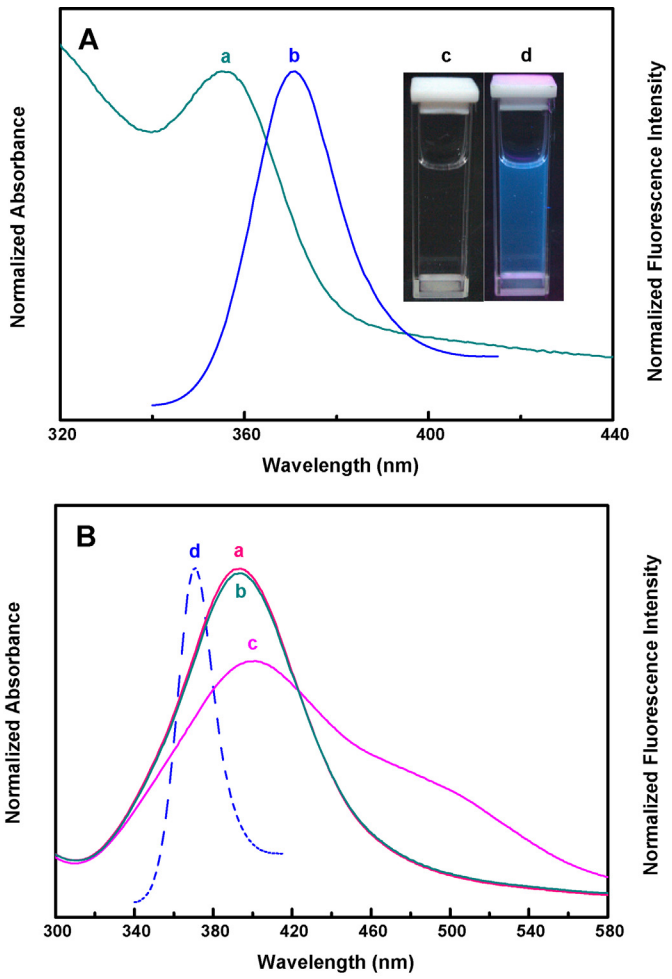

Fig. 1. (A) The normalized UV–vis absorption (a) and fluorescence emission (b) spectra of 0.17 mM ZnSe QDs; the digital photographs of 0.17 mM ZnSe QDs solution under visible light (c) and a 308 nm UV lamp (d). (B) The normalized absorption spectra of 1.3 nM AgNPs in the absence (a), 18 $\mu g\,L^{-1}$ (b) and 3.0×10^4 $\mu g\,L^{-1}$ (c) of melamine; the normalized fluorescence emission spectrum of 0.17 mM ZnSe QDs (d).

spectrum band is very narrow with the full width at half-maximum (FWHM) about 25 nm, which reveals that the as-prepared QDs are of good size homogeneity. ZnSe QDs solution was colorless and transparent under visible light (c in Fig. 1A) and could emit bright blue fluorescence under excitation at a 308 nm UV lamp (d in Fig. 1A). According to a previously reported method [41], the QY of ZnSe QDs was calculated to be 28.6% at 370 nm with L-tryptophan as a reference. ζ of ZnSe QDs was measured to be −64.3 mV at pH 8 (Fig. S1A), due to the deprotonation of the —COOH in L-GSH (pI = 5.93) [46].

The UV–vis absorption spectrum of as-prepared citrate-stabilized AgNPs was recorded in the wavelength range from 300 to 580 nm (a in Fig. 1B). The yellow AgNPs colloid displays a strong characteristic surface plasmon absorption peak around 395 nm. A typical HRTEM image indicates that AgNPs are monodisperse (Fig. 2A) and the particles shape is near-spherical (inset 1 in Fig. 2A). The selected area electron diffraction (SAED) pattern of AgNPs (inset 2 in Fig. 2A) demonstrates the mono-crystalline nature of these NPs. ζ of AgNPs was measured to be -34.3 mV at pH 8 (Fig. S1B). Owing to the strong electrostatic repulsion among the negatively charged capping agents (citrate ions) against van der Waals attraction, the yellow AgNPs colloid can be effectively stabilized against aggregation for several months. As shown in Fig. 1B, it is obvious that the emission spectrum of ZnSe QDs (d) can overlap

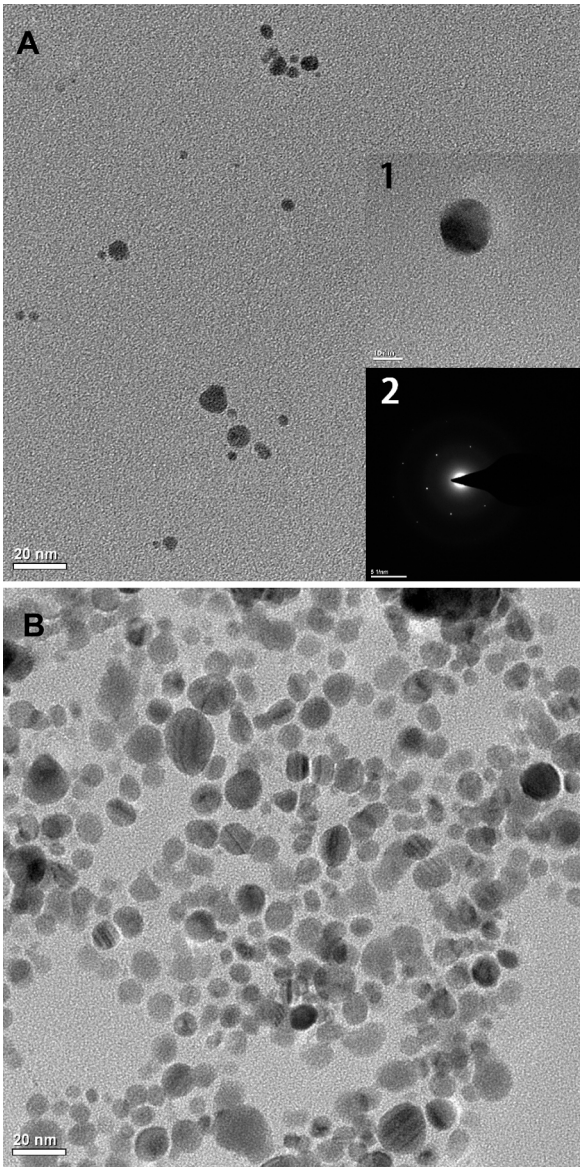

Fig. 2. TEM images of 1.3 nM AgNPs in the absence (A) and presence (B) of 3.0×10^4 μg L^{-1} melamine. Inset 1 in (A): a HRTEM image for a single Ag nanoparticle; inset 2 in (A): The SAED pattern of AgNPs.

with the absorption spectrum of AgNPs (a) to some extent, suggesting that IFE might take place with ZnSe QDs as fluorophore and AgNPs as absorber. Thus, if ZnSe QDs and AgNPs coexist, the fluorescence emission of ZnSe QDs might be obviously weakened or even substantially quenched by AgNPs with a high ε.

3.2. The IFE of AgNPs on the fluorescence emission of the ZnSe QDs

It can be seen from Fig. 3 that the fluorescence emission intensity of ZnSe QDs is efficiently quenched by AgNPs in a concentration-dependent way. Since both ZnSe QDs and AgNPs were strongly negatively charged, it could be deduced that there was a strong electrostatic repulsion effect between them, and no electrostatic attraction-induced FRET donor-accepter assemblies could form [25]. A hydrogen bond-based FRET pair could also hardly be established as —COOH in citric acid were entirely deprotonated at pH 8 [47]. Fluorescence lifetime measurement was conducted to confirm the fluorescence quenching mechanism since IFE and static quenching are deemed to have no effect on the excitation lifetime

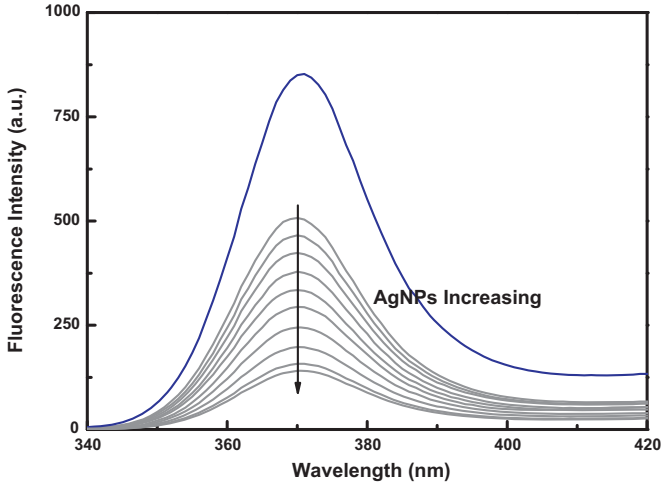

Fig. 3. The fluorescence emission spectra of ZnSe QDs in the presence of increasing concentrations of AgNPs. The concentration of AgNPs is 0, 0.13, 0.26, 0.39, 0.52, 0.65, 0.78, 0.91, 1.04, 1.17 and 1.3 nM, respectively; ZnSe QDs, 0.17 mM.

of the fluorophore. As shown in Fig. S2, the fluorescence decay curve of ZnSe QDs has no change in the absence and presence of AgNPs, which verified that no available FRET process has occurred. Moreover, the fact that plasmon absorption band of AgNPs showed no obvious variation in the absence (a) and presence (b) of ZnSe QDs (Fig. S3), which further indicated that no complex has formed between them. Therefore, all these results synthetically manifested that the fluorescence decrease was mostly ascribed to the IFE of AgNPs on the fluorescence emission of ZnSe QDs.

Significantly, owing to the high ε of AgNPs, the fluorescence emission intensity of 0.17 mM ZnSe QDs at 370 nm decreased by more than 83% in the presence of 1.3 nM AgNPs (Fig. 3). Thus the fluorescence emission of ZnSe QDs at 370 nm can be easily tuned by the absorbance change of AgNPs, which offers a decent fluorescence "off-state" for the following sensitive "turn-on" analysis.

3.3. Interaction between melamine and AgNPs

It has been well known that characteristic absorption peaks of AuNPs and AgNPs are closely related with interparticle distance [17]. When monodisperse AuNPs or AgNPs approach to each other and tend to aggregate upon external inducement, the interparticle distance will gradually decrease. In consequence, original characteristic absorption peaks of AuNPs or AgNPs will display a distinct red shift, accompanied by corresponding absorbance and solution color changes [17]. The melamine-induced changes of absorption spectrum of AgNPs are shown in Fig. 1B. 1.3 nM well-dispersed AgNPs exhibited a strong absorption peak at 395 nm (a in Fig. 1B). In the presence of a low concentration of melamine (18 μg L^{-1}), only slight variation was observed in the absorption spectrum (b in Fig. 1B). However, upon addition of a high concentration of melamine (3.0×10^4 μg L^{-1}), the absorbance of AgNPs at 395 nm significantly decreased, and there appeared a new absorption peak in the long-wavelength band (~500 nm) (c in Fig. 1B). TEM result further confirmed that AgNPs aggregation was induced by melamine (Fig. 2B), which resulted in a conspicuous change of solution color from yellow to red and the corresponding spectrum variation.

In fact, this colorimetric strategy had been applied for visual melamine sensing in our previous work [23]. As shown in (3) in Scheme 1C, melamine can intensively attach to AgNPs surface through its amine groups by ligand exchange with citrate ions, which will cripple the electrostatic repulsion among AgNPs, decreasing the colloid stability and finally resulting in the

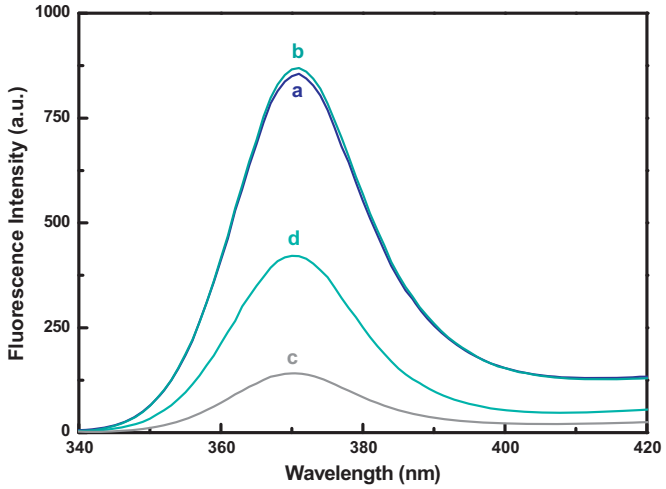

Fig. 4. The fluorescence emission spectra of 0.17 mM ZnSe QDs (a), 0.17 mM ZnSe QDs mixed with 3.0×10^4 μg L^{-1} melamine (b), 0.17 mM ZnSe QDs mixed with 1.3 nM AgNPs (c) and 0.17 mM ZnSe QDs mixed with 1.3 nM AgNPs and 18 μg L^{-1} melamine (d).

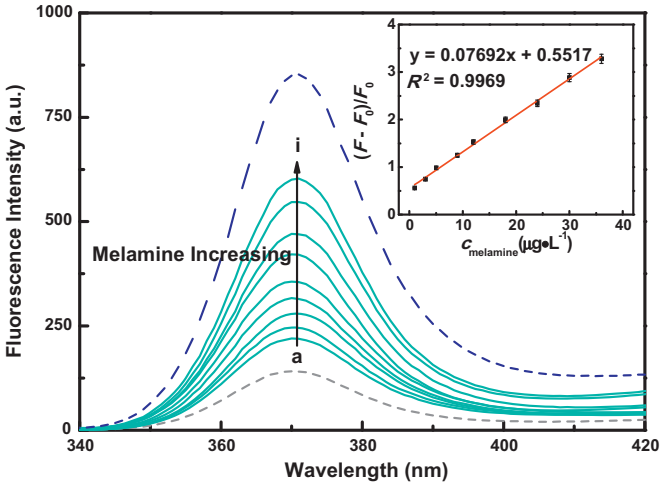

Fig. 5. The fluorescence emission spectra of the AgNPs–ZnSe detection system in the presence of increasing concentrations of melamine. The inset shows the linear calibration plot of $(F-F_0)/F_0$ *versus* melamine concentration. The melamine concentration (solid curves, *a–i*) is 1, 3, 5, 9, 12, 18, 24, 30 and 36 μg L^{-1}, respectively. AgNPs, 1.3 nM; ZnSe QDs, 0.17 mM.

aggregation of AgNPs. Hydrogen bonds among melamine molecules can also accelerate the aggregation process due to their molecular crosslinking effect. Unfortunately, this method could only display a low sensitivity with a detection limit of 231 μg L^{-1}. Herein, melamine can effectively modulate the spectrum overlap between the absorption band of AgNPs and the emission band of ZnSe QDs (Fig. 1B). Thus, if we establish an IFE-based assay through the modulation effect, an enhanced sensitivity for melamine detection could be expected.

3.4. Fluorescence response of IFE-based assay for melamine

To validate the expected detecting performance, the fluorescence response of the IFE-based assay for melamine was further investigated (Fig. 4). The fluorescence emission spectra of 0.17 mM ZnSe QDs show no obvious difference in the absence (a in Fig. 4) and presence (b in Fig. 4) of 3.0×10^4 μg L^{-1} melamine, which indicates that even if a relatively high concentration of melamine was added, no considerable fluorescence variation of ZnSe QDs would appear. When 0.17 mM ZnSe QDs was mixed with 1.3 nM AgNPs, the fluorescence emission was effectively quenched *via* IFE (c in Fig. 4). However, with the presence of 18 μg L^{-1} melamine, the IFE-decreased fluorescence significantly recovered (d in Fig. 4). No noticeable change of spectral shape was observed, which demonstrated that no new fluorescent center emerged and the recovered fluorescence was still derived from ZnSe QDs. Thus, it was confirmed that the fluorescence recovery should completely originate from the interaction between melamine and AgNPs, which modulated the IFE and further influenced the fluorescence emission of ZnSe QDs. It can be clearly seen that a higher sensitivity was obtained compared with the above-mentioned colorimetric strategy.

3.5. Optimization of experimental conditions

In the proposed assay for melamine, the fluorescence recovery of ZnSe QDs is highly pH-dependent. Melamine is a weak base with a pK_a of 5.05, and media pH also influences the form of melamine molecules in aqua phase. Herein, using 0.1 M NaOH or HCl for pH adjustment, the influence of different pH on $(F-F_0)/F_0$ for the detection of 18 μg L^{-1} melamine was investigated in the pH range from 5 to 10 (Fig. S4). It could be observed that the highest $(F-F_0)/F_0$ value was obtained at pH 8. On one hand, in strong acid or alkali media, melamine will hydrolyze, and its amino groups will be gradually displaced by hydroxyl groups [4]. Then melamine will finally transform into cyanuric acid that cannot induce the aggregation of AgNPs [23]. Hence a near-neutral pH must be adopted to avoid melamine hydrolysis in this assay. On the other hand, a more sensitive interaction between melamine and AgNPs may be achieved at pH 8 [23], which could better adjust the IFE process. So, the optimal pH 8 was chosen throughout this study.

The influence of the AgNPs concentration on the fluorescence recovery was also studied. As shown in Fig. S5, in the presence of 18 μg – L^{-1} melamine, $(F-F_0)/F_0$ rose gradually with an increasing concentration of AgNPs until the AgNPs concentration reached to 1.3 nM. Then $(F-F_0)/F_0$ would decrease if the AgNPs concentration continued to increase. This is because when a relatively low concentration of AgNPs was adopted, the corresponding background fluorescence would be too strong to display a wider linear range. Besides, when the AgNPs concentration goes beyond 1.3 nM, melamine molecules cannot thoroughly replace citrate ions on the AgNPs surface, resulting in poor sensitivity for melamine. Therefore, 1.3 nM was chosen to be the optimal AgNPs concentration.

The effect of reaction time was further discussed. As shown in Fig. S6, after 3.0×10^4 μg L^{-1} melamine was added, the absorbance of the 1.3 nM AgNPs at 395 nm gradually decreased as time went on, and the aggregation of AgNPs could almost complete within 16 min. Moreover, IFE can be generally considered as a kind of instant effect. Therefore, the reaction time of melamine-AgNPs binding was adopted as 16 min, and no extra incubation was needed after the addition of ZnSe QDs.

3.6. Sensitivity and selectivity

Under the above-mentioned optimal conditions, the fluorescence emission spectra of ZnSe QDs in the presence of different concentrations of melamine were plotted in Fig. 5. It can be observed that the IFE-decreased fluorescence remarkably recovered with the gradual increase of melamine concentration. A decent linear relationship between $(F-F_0)/F_0$ and melamine concentration (the inset in Fig. 5) was observed in the range from 1.0 to 36 μg L^{-1} ($R^2 = 0.9969$). The detection limit was measured to be 0.11 μg L^{-1} ($S/N = 3$), which is far below the detection limit of HPLC in Chinese National Standard GB/T 22388-2008 [48] (0.6 mg kg^{-1}) and the safety limits regulated by the U.S. and China (2.5 mg kg^{-1} for

Table 1
Comparison of LODs of different melamine detecting methods.

Method	LOD ($\mu g\,L^{-1}$)	Ref.
HPLC	18	[5]
LC–MS/MS	8	[6]
GC–MS	20	[7]
ELISA	3.9	[8]
NIR	2×10^5	[9]
CZE	50	[10]
EC	1.21	[11]
CL	120	[12]
FL	19	[13]
SERS	10	[14]
PDA liposome-based colorimetry	500	[15]
AuNPs-based colorimetry	400	[22]
AgNPs-based colorimetry	231	[23]
AuNPs-CdTe FRET-based FL	0.67	[27]
AuNPs-CdS IFE-based FL	17	[32]
AgNPs-ZnSe IFE-based FL	0.11	This work

adult food and 1 mg kg^{-1} for infant formula). Compared with other methods (Table 1), the detection limit of this method is also quite competitive. The relative standard deviation (RSD) for 11 repeated measurements of 18 $\mu g\,L^{-1}$ melamine was 1.3%, which reveals satisfactory reproducibility of this method.

The selectivity of the method was evaluated by investigating the influence of various potential interfering substances on the fluorescence recovery. As shown in Table S1, it can be seen that for these substances with concentrations of 100-fold higher than that of coexisting melamine, the fluorescence intensity variations were less than ±5% and could hardly produce considerable interferences for melamine detection. Thus, the IFE-based assay exhibited a highly-selective fluorescence response to melamine and could be very promising for practical application.

3.7. Detection of melamine in real samples

To verify the practicality of this IFE-based assay, different concentrations of melamine were spiked into real milk and egg samples, and then the samples were handled and analyzed according to the procedures described in Section 2.6. As shown in Table 2, it can be seen that for melamine concentrations of 1.0, 5.0 and 25 $\mu g\,L^{-1}$, excellent recoveries ranging from 97.2 to 103.4% were achieved with variation coefficients (CV) of 0.7 to 3.7%. These results demonstrated that the "turn-on" fluorescence assay based on IFE was sensitive enough and very reliable for practical detection of melamine in raw milk and egg samples.

Table 2
Results of melamine detection in the real samples.

Sample	Spiked ($\mu g\,L^{-1}$)	Found ($\mu g\,L^{-1}$)[a]	Recovery (%)	RSD (%)
Raw milk 1	1.0	0.9731	97.3	2.6
	5.0	4.913	98.3	1.5
	25	24.78	99.1	1.9
Raw milk 2	1.0	0.9943	99.4	0.7
	5.0	4.966	99.3	3.7
	25	24.53	98.1	1.4
Raw milk 3	1.0	1.019	101.9	1.5
	5.0	5.067	101.3	0.8
	25	25.53	102.1	2.0
Egg 1	1.0	1.034	103.4	2.8
	5.0	4.908	98.2	3.1
	25	25.39	101.6	1.1
Egg 2	1.0	0.9721	97.2	2.4
	5.0	5.083	101.7	0.9
	25	25.21	100.8	1.7

[a] Mean of three measurements.

4. Conclusion

In summary, with eco-friendly L-GSH-capped ZnSe QDs as an ideal fluorophore and citrate-stabilized AgNPs as a powerful absorber, an efficient IFE-based "turn-on" fluorescence assay for melamine has been established in this study. Some important experimental factors which would affect the IFE efficiency and the interaction between melamine and AgNPs were optimized. The proposed method was successfully applied to detect melamine in raw milk and egg samples. Very low concentrations of melamine in the spiked samples were successfully detected, which is greatly lower than the detection limit of HPLC stipulated in GB/T 22388-2008 and the safety limits regulated by the U.S. and China. The method reveals many advantages, such as high sensitivity, easy operation, low cost and eco-friendliness, which makes it to be a very promising choice for on-site and real-time screening of melamine.

Acknowledgments

This work was financially supported by the National Natural Science Foundation of China (No. 20905031), the Natural Science Foundation of Jilin Province (No. 201215024) and Innovation Projects of Science Frontiers and Interdisciplinary of Jilin University.

Appendix A. Supplementary data

Supplementary data associated with this article can be found, in the online version, at http://dx.doi.org/10.1016/j.snb.2014.06.056.

References

[1] F.X. Sun, W. Ma, L.G. Xu, Y.Y. Zhu, L.Q. Liu, C.F. Peng, L.B. Wang, H. Kuang, C.L. Xu, Analytical methods and recent developments in the detection of melamine, Trends Anal. Chem. 29 (2010) 1239–1249.
[2] Y.Q. Chen, W.J. Yang, Z.Y. Wang, Y. Peng, B. Li, L.Y. Zhang, L.M. Gong, Deposition of melamine in eggs from laying hens exposed to melamine contaminated feed, J. Agric. Food Chem. 58 (2010) 3512–3516.
[3] T. Kobayashi, A. Okada, Y. Fujii, K. Niimi, S. Hamamoto, T. Yasui, K. Tozawa, K. Kohri, The mechanism of renal stone formation and renal failure induced by administration of melamine and cyanuric acid, Urol. Res. 38 (2010) 117–125.
[4] J.L. Dorne, D.R. Doerge, M. Vandenbroeck, J. Fink-Gremmels, W. Mennes, H.K. Knutsen, F. Vernazza, L. Castle, L. Edler, D. Benford, Recent advances in the risk assessment of melamine and cyanuric acid in animal feed, Toxicol. Appl. Pharmacol. 270 (2013) 218–229.
[5] H.W. Sun, L.X. Wang, L.F. Ai, S.X. Liang, H. Wu, A sensitive and validated method for determination of melamine residue in liquid milk by reversed phase high-performance liquid chromatography with solid-phase extraction, Food Control 21 (2010) 686–691.
[6] P.C. Wang, R.J. Lee, C.Y. Chen, C.C. Chou, M.R. Lee, Determination of cyromazine and melamine in chicken eggs using quick, easy, cheap, effective, rugged and safe (QuEChERS) extraction coupled with liquid chromatography-tandem mass spectrometry, Anal. Chim. Acta 752 (2012) 78–86.
[7] X.D. Pan, P.G. Wu, D.J. Yang, L.Y. Wang, X.H. Shen, C.Y. Zhu, Simultaneous determination of melamine and cyanuric acid in dairy products by mixed-mode solid phase extraction and GC–MS, Food Control 30 (2013) 545–548.
[8] B.Y. Cao, H. Yang, J. Song, H.F. Chang, S.Q. Li, A.P. Deng, Sensitivity and specificity enhanced enzyme-linked immunosorbent assay by rational hapten modification and heterogeneous antibody/coating antigen combinations for the detection of melamine in milk, milk powder and feed samples, Talanta 116 (2013) 173–180.
[9] X.P. Fu, M.S. Kim, K.L. Chao, J.W. Qin, J. Lim, H. Lee, A. Garrido-Varo, D. Pérez-Marín, Y.B. Ying, Detection of melamine in milk powders based on NIR hyperspectral imaging and spectral similarity analyses, J. Food Eng. 124 (2014) 97–104.
[10] J.G. Xia, N.Y. Zhou, Y.J. Liu, B. Chen, Y.N. Wu, S.Z. Yao, Simultaneous determination of melamine and related compounds by capillary zone electrophoresis, Food Control 21 (2010) 912–918.
[11] Q.A. Cao, H. Zhao, L.X. Zeng, J. Wang, R. Wang, X.H. Qiu, Y.J. He, Electrochemical determination of melamine using oligonucleotides modified gold electrodes, Talanta 80 (2009) 484–488.
[12] H.J. Zeng, R. Yang, Q.W. Wang, J.J. Li, L.B. Qu, Determination of melamine by flow injection analysis based on chemiluminescence system, Food Chem. 127 (2011) 842–846.

[13] H. Huang, L. Li, Q. Ma, Y.Q. Feng, Z.K. He, Determination of melamine in milk by fluorescent spectrophotometry with cetyltrimethylammonium bromide, Chin. J. Anal. Chem. 38 (2010) 249–252.
[14] X.F. Zhang, M.Q. Zou, X.H. Qi, F. Liu, X.H. Zhu, B.H. Zhao, Detection of melamine in liquid milk using surface-enhanced Raman scattering spectroscopy, J. Raman Spectrosc. 41 (2010) 1655–1660.
[15] J. Lee, E.J. Jeong, J. Kim, Selective and sensitive detection of melamine by intra/inter liposomal interaction of polydiacetylene liposomes, Chem. Commun. 47 (2011) 358–360.
[16] K. Saha, S.S. Agasti, C. Kim, X.N. Li, V.M. Rotello, Gold nanoparticles in chemical and biological sensing, Chem. Rev. 112 (2012) 2739–2779.
[17] D. Vilela, M.C. González, A. Escarpa, Sensing colorimetric approaches based on gold and silver nanoparticles aggregation: chemical creativity behind the assay. A review, Anal. Chim. Acta 751 (2012) 24–43.
[18] S.Y. Lin, S.W. Liu, C.M. Lin, C.H. Chen, Recognition of potassium ion in water by 15-crown-5 functionalized gold nanoparticles, Anal. Chem. 74 (2002) 330–335.
[19] S.Y. Lin, S.H. Wu, C.H. Chen, A simple strategy for prompt visual sensing by gold nanoparticles: general applications of interparticle hydrogen bonds, Angew. Chem. Int. Ed. 45 (2006) 4948–4951.
[20] K. Aslan, J.R. Lakowicz, C.D. Geddes, Nanogold-plasmon-resonance-based glucose sensing, Anal. Biochem. 330 (2004) 145–155.
[21] J. Matsui, K. Akamatsu, S. Nishiguchi, D. Miyoshi, H. Nawafune, K. Tamaki, N. Sugimoto, Composite of Au nanoparticles and molecularly imprinted polymer as a sensing material, Anal. Chem. 76 (2004) 1310–1315.
[22] X.S. Liang, H.P. Wei, Z.Q. Cui, J.Y. Deng, Z.P. Zhang, X.Y. You, X.E. Zhang, Colorimetric detection of melamine in complex matrices based on cysteamine-modified gold nanoparticles, Analyst 136 (2011) 179–183.
[23] H. Ping, M.W. Zhang, H.K. Li, S.G. Li, Q.S. Chen, C.Y. Sun, T.H. Zhang, Visual detection of melamine in raw milk by label-free silver nanoparticles, Food Control 23 (2012) 191–197.
[24] R. Gill, M. Zayats, I. Willner, Semiconductor quantum dots for bioanalysis, Angew. Chem. Int. Ed. 47 (2008) 7602–7625.
[25] X. Wang, X.Q. Guo, Ultrasensitive Pb^{2+} detection based on fluorescence resonance energy transfer (FRET) between quantum dots and gold nanoparticles, Analyst 134 (2009) 1348–1354.
[26] E. Oh, M.Y. Hong, D. Lee, S.H. Nam, H.C. Yoon, H.S. Kim, Inhibition assay of biomolecules based on fluorescence resonance energy transfer (FRET) between quantum dots and gold nanoparticles, J. Am. Chem. Soc. 127 (2005) 3270–3271.
[27] F. Gao, Q.Q. Ye, P. Cui, L. Zhang, Efficient fluorescence energy transfer system between CdTe-doped silica nanoparticles and gold nanoparticles for turn-on fluorescence detection of melamine, J. Agric. Food Chem. 60 (2012) 4550–4558.
[28] M. Massey, W.R. Algar, U.J. Krull, Fluorescence resonance energy transfer (FRET) for DNA biosensors: FRET pairs and Förster distances for various dye-DNA conjugates, Anal. Chim. Acta 568 (2006) 181–189.
[29] W.Y. Ji, P.T. Jing, W. Xu, X. Yuan, Y.J. Wang, J.L. Zhao, A.K.Y. Jen, High color purity ZnSe/ZnS core/shell quantum dot based blue light emitting diodes with an inverted device structure, Appl. Phys. Lett. 103 (2013) 053106.
[30] P. Yuan, D.R. Walt, Calculation for fluorescence modulation by absorbing species and its application to measurements using optical fibers, Anal. Chem. 59 (1987) 2391–2394.
[31] Q. Zhang, Y.Y. Qu, M. Liu, X.L. Li, J.T. Zhou, X.W. Zhang, H. Zhou, A sensitive enzyme biosensor for catecholics detection via the inner filter effect on fluorescence of CdTe quantum dots, Sens. Actuators B 173 (2012) 477–482.
[32] X.Y. Cao, F. Shen, M.W. Zhang, J.J. Guo, Y.L. Luo, X. Li, H. Liu, C.Y. Sun, J.B. Liu, Efficient inner filter effect of gold nanoparticles on the fluorescence of CdS quantum dots for sensitive detection of melamine in raw milk, Food Control 34 (2013) 221–229.
[33] J.W. Li, X.M. Li, X.J. Shi, X.W. He, W. Wei, N. Ma, H. Chen, Highly sensitive detection of caspase-3 activities via a nonconjugated gold nanoparticle-quantum dot pair mediated by an inner-filter effect, ACS Appl. Mater. Interfaces 5 (2013) 9798–9802.
[34] L. Shang, S.J. Dong, Design of fluorescent assays for cyanide and hydrogen peroxide based on the inner filter effect of metal nanoparticles, Anal. Chem. 81 (2009) 1465–1470.
[35] N. Shao, Y. Zhang, S.M. Cheung, R.H. Yang, W.H. Chan, T. Mo, K.A. Li, F. Liu, Copper ion-selective fluorescent sensor based on the inner filter effect using a spiropyran derivative, Anal. Chem. 77 (2005) 7294–7303.
[36] J.S. Lee, A.K.R. Lytton-Jean, S.J. Hurst, C.A. Mirkin, Silver nanoparticle-oligonucleotide conjugates based on DNA with triple cyclic disulfide moieties, Nano Lett. 7 (2007) 2112–2115.
[37] A. Moores, F. Goettmann, The plasmon band in noble metal nanoparticles: an introduction to theory and applications, New J. Chem. 30 (2006) 1121–1132.
[38] J.J. Andrade, A.G. Brasil Jr., P.M.A. Farias, A. Fontes, B.S. Santos, Synthesis and characterization of blue emitting ZnSe quantum dots, Microelectron. J. 40 (2009) 641–643.
[39] J. Wang, T.J. Mountziaris, Homogeneous immunoassays based on fluorescence emission intensity variations of zinc selenide quantum dot sensors, Biosens. Bioelectron. 41 (2013) 143–149.
[40] Y.G. Zheng, Z.C. Yang, J.Y. Ying, Aqueous synthesis of glutathione-capped ZnSe and $Zn_{1-x}Cd_xSe$ alloyed quantum dots, Adv. Mater. 19 (2007) 1475–1479.
[41] J.R. Lakowicz, Principles of Flourescence Spectroscopy, 3rd ed., Kluwer Academic/Plenum Publishers, New York, 2006, pp. 54–55.
[42] S. Deka, A. Quarta, M.G. Lupo, A. Falqui, S. Boninelli, C. Giannini, G. Morello, M. De Giorgi, G. Lanzani, C. Spinella, R. Cingolani, T. Pellegrino, L. Manna, CdSe/CdS/ZnS double shell nanorods with high photoluminescence efficiency and their exploitation as biolabeling probes, J. Am. Chem. Soc. 131 (2009) 2948–2958.
[43] S. Dhami, A.J. De Mello, G. Rumbles, S.M. Bishop, D. Phillips, A. Beeby, Phthalocyanine fluorescence at high concentration: dimers or reabsorption effect, Photochem. Photobiol. 61 (1995) 341–346.
[44] R.C. Doty, T.R. Tshikhudo, M. Brust, D.G. Fernig, Extremely stable water-soluble Ag nanoparticles, Chem. Mater. 17 (2005) 4630–4635.
[45] J.R.G. Navarro, M.H.V. Werts, Resonant light scattering spectroscopy of gold, silver and gold–silver alloy nanoparticles and optical detection in microfluidic channels, Analyst 138 (2013) 583–592.
[46] Y.Z. Shen, S.P. Liu, P.F. Yin, Y.Q. He, Interaction of herring sperm DNA with lomefloxacin hydrochloride-Cu(II) based on changes in the fluorescence intensity of GSH-CdTe/CdS quantum dots, Chem. J. Chin. Univ. 34 (2013) 1360–1367.
[47] M. Xue, X. Wang, H. Wang, D.Z. Chen, B. Tang, Hydrogen bond breakage by fluoride anions in a simple CdTe quantum dot/gold nanoparticle FRET system and its analytical application, Chem. Commun. 47 (2011) 4986–4988.
[48] GB/T 22388-2008, Determination of Melamine in Raw Milk and Dairy Products, Standards Press of China, Beijing, 2003.

Biographies

Xianyi Cao received his B.Sc. in chemical engineering from Harbin Institute of Technology (2008). He is currently an M.Sc. student of Jilin University in food science. His research interests focus on synthesis of nanomaterials and their application in food safety.

Fei Shen was born on December 10, 1990 and received her B.Sc. in food quality and safety from Jilin University (2012). She is currently an M.Sc. student of Jilin University in food science. Her research interests cover synthesis of nanomaterials and their application in food safety.

Minwei Zhang received his M.Sc. degree in food science from Jilin University (2013). He is now a Ph.D. student of Technical University of Denmark in nanochemistry. His research interests cover nano-based biosensors.

Chunyan Sun received her Ph.D. degree in analytical chemistry at Chang Chun Institute of Applied Chemistry, Chinese Academy of Sciences (2006). She is a professor of food quality and safety at Jilin University, Changchun, China. Her research interests cover biosensors and their application in food safety.